Hydrogel Actuator with a Built-In Stimulator Using Liquid Metal for Local Control

Ken Matsubara, Daiki Tachibana, Ryosuke Matsuda, Hiroaki Onoe, Ohmi Fuchiwaki, and Hiroki Ota*

Hydrogel actuators, comprising gels that convert external stimuli into mechanical motion for actuation, are attracting attention for their promising applications, such as in robotics. The driving force is the absorption or release of water or another solvent, which results in swelling and shrinking motions, leading in turn to more complex functionalities. However, practical hydrogel actuators that can be controlled locally, such as ones that allow local actuation around the joints in rigid-bodied robots, do not exist. Herein, the driving target of a thermo-responsive hydrogel, poly(*N*-isopropyl acrylamide), is integrated with the stimulation module using a liquid metal. The stimulation module provides heat as an external stimulus to the hydrogel actuator. The motion of the actuator is triggered by the heat supplied by an ultrasoft hydrogel coil, with liquid metal surrounding the driving target. The heat generated by current flowing through the liquid metal changes the temperature only around the desired part of the actuator, which enables the electrical control of an individual part of the hydrogel actuator. The concept of integrating the driving target and stimulator is expected to facilitate functional movement of actuators and expand the range of potential applications of hydrogels.

Stimuli-responsive materials such as shape memory alloys, dielectric polymers, and electroactive polymers can convert various external stimuli such as electricity, chemicals, light, pH, and heat into repeatable and controllable shape transformations.[1–10] Of these materials, hydrogels are considerably softer

K. Matsubara, D. Tachibana, R. Matsuda, Dr. O. Fuchiwaki, Dr. H. Ota
Department of Mechanical Engineering
Yokohama National University
79-5 Tokiwadai, Hodogaya-ku, Yokohama 240-8501, Japan
E-mail: ota-hiroki-xm@ynu.ac.jp

Dr. H. Onoe
Department of Mechanical Engineering
Keio University
3-14-1 Hiyoshi, Kohoku-ku, Yokohama 223-8522, Japan

Dr. O. Fuchiwaki, Dr. H. Ota
Graduate School of System Integration
Yokohama National University
79-5 Tokiwadai, Hodogaya-ku, Yokohama 240-8501, Japan

The ORCID identification number(s) for the author(s) of this article can be found under https://doi.org/10.1002/aisy.202000008.

and wetter than any other material. As a result, they have attracted much attention and appeal for use in promising applications such as drug delivery systems (DDS),[11–13] artificial muscles,[14,15] tissue engineering,[16] and microactuators.[17,18] The hydrogels consist of 3D polymer networks with a strong water absorption ability and these materials show high functionality for swelling or shrinking.[19] In this respect, the behavior of hydrogels mimics the hydromorphic movement of plants and animals,[20–23] such as shrinking, bending, and twisting, which render small and soft actuators with the advantages of possessing a soft touch, simplicity in operation, and being waterproof.

The driving forces of the hydrogel actuators are based on the absorption and release of water. The movements governed by these driving forces can be triggered by external physical or chemical stimuli, such as electricity, light, magnetic field, heat, gases, and organic solvents. The approaches used to realize the desired movements and deformations are twofold: applying an external nonuniform stimulus[24–26] or arranging internal anisotropic hydrogels.[27–31] Using these methods, complex movements such as folding, walking, and expanding have been achieved.[32,33] Typically, a change in environmental conditions causes homogeneous expansion or contraction of homogeneous hydrogels in all directions, whereas inhomogeneous hydrogels can realize more complex movements, such as walking.[34] However, to actuate both types of hydrogels, the environment of the entire area or chamber containing the gel actuator needs to be controlled. In other words, factors that trigger the driving forces, such as pH or temperature, should be applied to the whole field where the actuators exist.[35] This requires the expense of enormous amounts of energy, apart from the difficulties with more complicated actuation which are associated with local control of the movements.

In conventional rigid-bodied robots, actuators realize complicated movements via the robot joints by controlling the movement of each joint locally. This enables multiaxis actuation of these rigid robots. To establish local control of the hydrogel actuators, a near-infrared (nIR) laser spot is used as external stimulation. The laser spot heats part of a hydrogel actuator and increases the temperature locally.[36,37] Despite the limited scope of application, this method is one of the most promising

**ADVANCED
SCIENCE NEWS**

www.advancedsciencenews.com

**ADVANCED
INTELLIGENT
SYSTEMS**
Open Access

www.advintellsyst.com

techniques for the local control of actuation. Laser stimulation cannot be used for hydrogel actuators inside colored liquids or cell culture medium liquids, because such liquids prevent the penetration of the laser. In addition, this method requires large equipment and high-performance lasers located outside the field of application. Therefore, there are no practical hydrogel actuators that can be controlled locally, despite this being a key potential technology to extend the types of movement and hence the range of applications of the hydrogel actuator.

The problem with achieving local control is that the driving target and the external stimulus module exist separately; thus, the entire area or field requires stimulation for actuation, thereby limiting the area that can be used with actuators. Therefore, to realize local control, which is required to perform multiple movements such as bending and shrinking independently in a single actuator, both the driving target for actuation and the stimulator that provides the stimulus to the driving target should be integrated or assembled into the hydrogel actuator. In this work, we propose a thermoresponsive gel actuator in which the stimulator is integrated using liquid metal, which provides a thermal stimulus to the actuators. For the stimulator, a resistive heater made of a liquid-metal hydrogel spring is used in this actuator. The spring surrounds the rod of the thermoresponsive gel, poly(N-isopropyl acrylamide) (PNIPAM), as the driving part. PNIPAM is one of the most attractive polymers for this application, as it causes large deformation in the hydrogel volume for small temperature changes. PNIPAM releases water inside the polymer above the lower critical solution temperature (LCST). Conversely, the polymer absorbs water from the environment to return to the original state. The resistive heating generated by the current flowing through the liquid metal can drive the shrinkage of the rod. Bending motion is achieved by taking advantage of the bilayered structure of the non-thermoresponsive and thermoresponsive gel (**Figure 1**a). Although the actual trigger of the hydrogel actuation is temperature, the actuation is controlled by electricity. Electrical control simplifies the operation and control of the actuator, in comparison with other
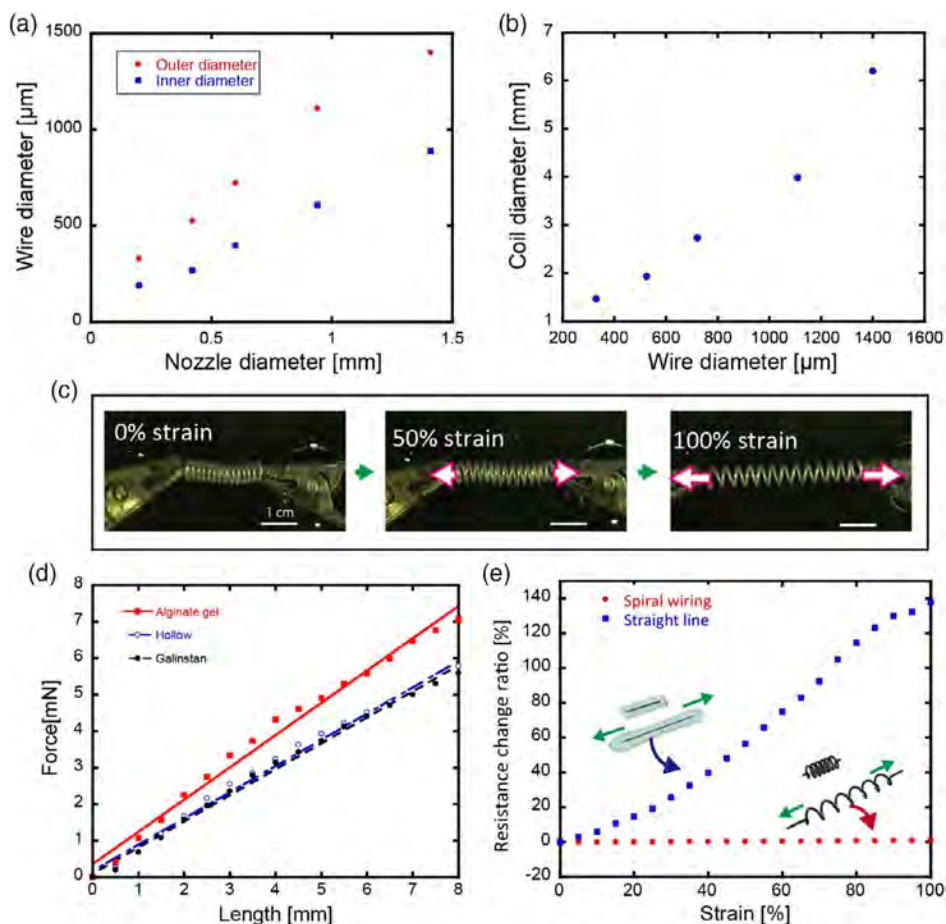
external stimuli. In addition, this hydrogel spring structure for the stimulator does not prevent the movement of the PNIPAM actuator, due to its ultrasoftness and the stretchability of the hydrogel spring. In this article, we focus on the local expansion of the gel actuator to realize individual actuation and demonstrate functional motions by a combination of actuators to show the feasibility of newly proposed gel actuators through experimental results found for basic motions such as expansion, contraction, and bending.

The liquid metal spring was fabricated by a combination of the bevel-tip nozzle method for the spring structure and a double bevel-tip nozzle method for the core–shell structure (Figure 1b(i)).[38] A helical structure of hydrogel was formed by the imbalance of crosslinking due to the inclination of the nozzle. The core–shell structure of the hydrogel was created by double nozzles held by a 3D-printed nozzle joint. In this study, polyvinyl alcohol (PVA) aqueous solution was used for the core part and sodium alginate for the shell part. Finally, the PVA solution was extruded by injecting the liquid metal, Galinstan (Figure S1, Supporting Information), and a hydrogel rod based on the PNIPAM gel was used for the actuation. The aqueous pregel solution was injected into the 3D-printed molds. The rod was detached from the mold (Figure 1b(ii)). In the case of the bilayer structure, the structure was established by polymerizing PNIPAM on the non-thermoresponsive gel, Alginate (Figure S2, Supporting Information). These two components, the liquid metal spring and thermoresponsive hydrogel rod, were integrated into the hydrogel actuator.

During the fabrication of the liquid metal spring, the nozzle size was altered from 0.20 to 1.41 mm. Meanwhile, the ratio of the volumetric flow rates of the shell and core sections was maintained at 4:1. As shown in **Figure 2**a, the wire diameters of the inner and outer structures increase with respect to the nozzle diameters. The diameters were controlled between 330 and 1111 µm. Similarly, the spring diameter increases with increasing nozzle diameter, as shown in Figure 2b. Figure 2c,d shows the measurement results of the spring constant for three
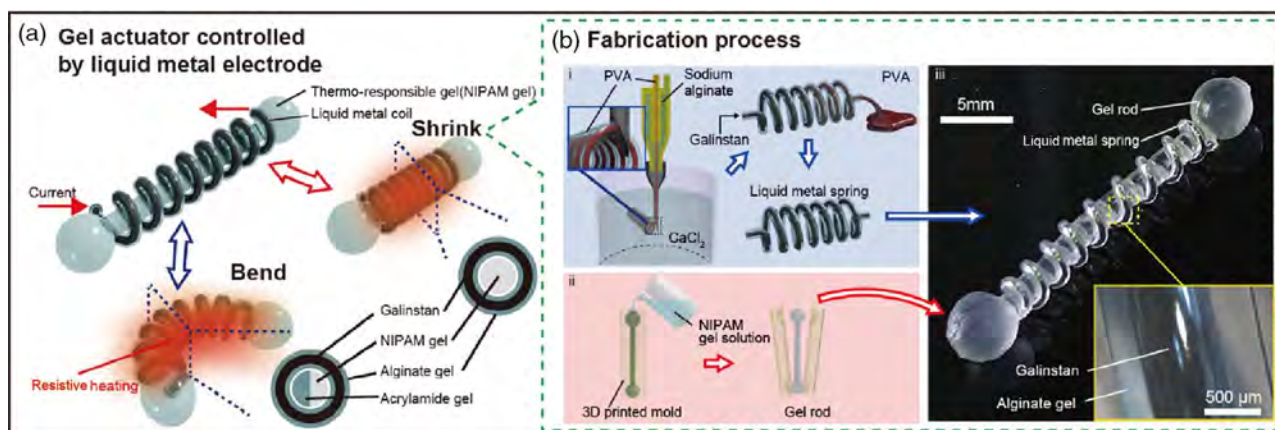
Figure 1. Hydrogel actuator integrated the rod of thermoresponsive gel and liquid metal spring. a) The actuator is composed of a PNIPAM hydrogel rod and a hydrogel spring with liquid metal. The driving part and stimulator for external stimuli are assembled in the actuator. The resistive heating by the liquid metal spring drives the actuator, which shrinks or bends the hydrogel rods with current control. b) The liquid metal spring is fabricated by a combination of the bevel-tip nozzle method for the spring structure and a double bevel-tip nozzle method for the core–shell structure. The hydrogel rod is molded using a 3D-printed mold, and both hydrogel components are assembled to form the actuator.

**ADVANCED
SCIENCE NEWS**

www.advancedsciencenews.com

**ADVANCED
INTELLIGENT
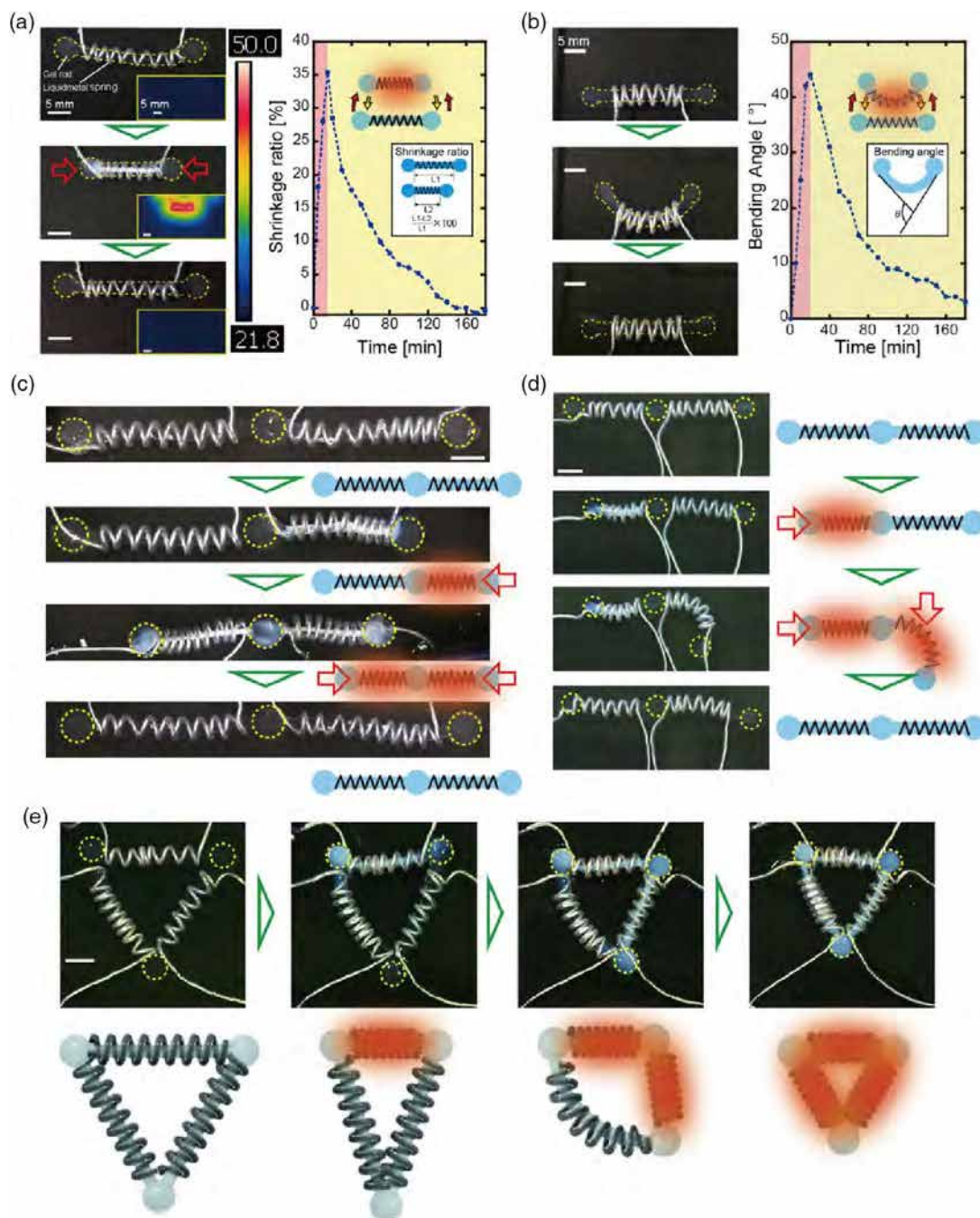SYSTEMS**
Open Access

www.advintellsyst.com

Figure 2. Mechanical and electrical characteristics of the hydrogel spring. a) Formed wire diameter with respect to the nozzle diameter. b) Formed coil diameter with respect to the nozzle diameter. c) Photographs of the spring strain up to 100%. d) Force change during the elongation of the hydrogel spring. e) Resistance change of a straight line and of a spiral wiring of liquid metal under strain.

different structures: a solid alginate spring, a hollow alginate spring, and an alginate spring with liquid metal inside. The spring was set on an electronic balance, and a weight was placed on the lower end and fixed (Figure S3a, Supporting Information). The spring constant was calculated from the length of the spring and its generative force. In the solid spring, the constant was 0.83 N m^{-1}. In the case of the springs having a hollow structure and a core–shell structure where the core part was filled with liquid metal, the constants were 0.72 and 0.71 N m^{-1}, respectively. Clearly, the constants of the hollow and core–shell structures were almost the same. In addition, the spring possesses good repeatability for mechanical deformations as shown in the repeatability test of Figure S3b, Supporting Information.

To observe the effect of the spring deformation during actuation due to its electrical properties, the resistance of the liquid metal was measured. As shown in Figure 2e, the resistance altered by only 1.2% under 100% strain. In contrast, the resistance of the straight channel filled with liquid metal increased by 137% under 100% strain. Also, the impedance of the liquid metal spring in alternating current (AC) was stable from 1 to 10^5 Hz (Figure S4, Supporting Information). From this, it was confirmed that the liquid metal spring has stable electrical

characteristics for both AC and DC. This resistance stability during deformation might lead to stability of control and actuator deformation.

Figure 3a shows shrinkage experiments of the telescopic actuator composed of a thermoresponsive gel rod and a liquid metal spring. As shown in Figure 3a, the shrinkage was correlated with the resistive heating of the liquid metal spring. The LCST of the PNIPAM gel was 32–35 °C and the temperature of the liquid metal coil increased to 50 °C. This is enough to activate the hydrophobic groups in PNIPAM, and shrinks the structure. The helical structure enables a uniform temperature increase inside the spring, as shown in the simulation based on COMSOL Multiphysics in Figure S5a, Supporting Information. In contrast, the straight channel of the liquid metal showed a significant temperature gradient inside the PNIPAM rod (Figure S5b, Supporting Information). The liquid metal spring can generate heating uniformly inside the structure and effectively supply heat to the thermoresponsive gel. In the first 15 min, the actuator shrank with a large deformation, reaching a shrinkage of 36%. The shrinkage of PNIPAM itself was 53% at 50 °C. However, the contraction of the gel rod was greater than the contraction of the spring when the spring shrank entirely.

**ADVANCED
SCIENCE NEWS**

www.advancedsciencenews.com

**ADVANCED
INTELLIGENT
SYSTEMS**

www.advintellsyst.com

Figure 3. Actuation of the hydrogel actuators. a) The actuator composed of a PNIPAM hydrogel rod and a spring with liquid metal. The temperature was increased from 22 to 50° at 3.5 W. b) The bending actuator composed of a bilayered rod of PNIPAM and acrylamide hydrogel. After turning off the current, both hydrogel actuators return to the original state. Local actuation of a dual actuator consisting of c) two telescopic actuators and d) telescopic and bending actuators. e) A triangle actuator composed of three telescopic actuators. A heated liquid metal spring locally controls the actuator using a current flow.

Therefore, the shrinkage ratio of the developed actuator was 36%. A compressive force of the actuator was caused by the thermoresponsive gel. The shrinkage of the gel spring was followed by the ends of the rod. After turning off the current, the PNIPAM gel gradually returned to its original size with the hydrogel spring. The liquid metal did not leak during the actuation. The surface

of the liquid metal is oxidized as soon as the surface is exposed to air or liquid, which increases surface tension. As a result, liquid metal did not leak from the hydrogel spring.

As shown in Figure S6, Supporting Information, the shrinkage of this actuator has good repeatability (the error was ±1.60% of the average shrinkage distance). The driving force

**ADVANCED
SCIENCE NEWS**

www.advancedsciencenews.com

**ADVANCED
INTELLIGENT
SYSTEMS**
Open Access

www.advintellsyst.com

of the thermoresponsive gel was calculated based on the spring constant of a gel spring (refer to Figure 2), as shown in Figure S7, Supporting Information. The resulting values for the driving force of the actuator, the force density, and the energy efficiency are 5.55 mN, 142 N m^{-3}, and 1.74×10^{-7}%, respectively. The functionality of the actuator was maintained for 3 months as long as the water in the container where the actuator was stored did not dry out.

In addition to the telescopic actuator, the bending actuator was developed using a rod made of a bilayer structure consisting of acrylamide and PNIPAM gel (Figure 3b). The PNIPAM section is able to shrink, and thus realize a bending movement due to the moment force generated by the contraction of the PNIPAM part. As shown in Figure 3b, the actuator deformed by 44° with the thermoresponsive gel after power had been supplied for 20 min. After turning off the current, the PNIPAM gel gradually returned to its original size.

For comparison with these results, similar experiments were conducted using an actuator surrounded by nichrome spring wiring with a diameter varying from 400 to 100 μm, as shown in Figure S8 and Table S1, Supporting Information. The interface between the nichrome and the PNIPAM rod seems to possess better adhesive properties than the one between the gel spring and the PNIPAM rod. However, the spring constant had such a high value that the driving force of the shrinkage of the actuator was withstood and the thermoresponsive gel was prevented from deforming. Wiring with a diameter smaller than 100 μm was difficult to form while maintaining the spring structure. Simultaneously, the resistance heating by the nichrome wire was transmitted to the rod via direct contact between the spring and the rod. As shown in the highly magnified image of Figure S8, Supporting Information, the temperature increase was not uniform because the wire was too fine. The gel spring was able to heat the entire area inside the spring, which implies that the efficiency of actuation might be improved. Therefore, the softness and adhesion of the liquid metal spring were found to be crucial to the shrinkage and bending motions of the thermoresponsive actuator.

Figure 3c shows an actuator connecting two telescopic actuators, which are composed entirely of PNIPAM and two liquid metal springs. The right section shrank when a current providing electrical power of 3.5 W was applied to the right spring (Figure 3c(i) and (ii)). After applying 3.5 W to the left spring, the left section shrank as well (Figure 3c(iii)). The actuator returned to the original state after turning off the current (Figure 3c(iv)). In the case of the combination of telescopic and bending actuators, as shown in Figure 3d(i)–(iv), each actuator of the telescopic and bending actuators was controlled by resistive heating of the liquid metal spring with current flow. As another demonstration, the triangle actuator composed of triple telescopic actuators was established, as shown in Figure 3d. The liquid metal spring shrank each of the actuators. Eventually, the size of the triangle decreased by 52% of its original size. Therefore, local control of the movement of the actuator driven by local resistive heating was achieved by the combination of a liquid metal spring and a thermoresponsive hydrogel (PNIPAM).

In this study, a locally controlled thermoresponsive gel actuator with an integrated driving target and stimulator for external stimulus was created. For the stimulator, a hydrogel spring filled with liquid metal was developed. The spring constant of the microsprings filled with liquid metal in the core parts was 0.71 N m^{-1} which indicates an ultrasoft property. Furthermore, the resistance of the spring was stable during its deformation. The telescopic actuator created by integrating this liquid metal spring and a thermoresponsive hydrogel rod contracted by 36% of the initial length. The bending actuator composed of the spring and a bilayered rod of acrylamide and PNIPAM bent through 44°. The softness of the spring and its electrical stability, coupled with a constant distance between the rod and the spring, realized locally controlled actuation of the thermoresponsive hydrogel with local heating of the liquid metal spring. Furthermore, in actuators made of dual and triple hydrogel rods based on PNIPAM, each actuator was controlled individually by the local current flow, which allows for more functional movement of the gel actuator and expands the potential for additional applications based on the hydrogel. As demonstrated, individual actuators in a single device were controlled individually simply via current flow, without needing large equipment. In addition, the actuators might be located inside the chamber, regardless of the liquid type, which leads to flexibility of the field during local control with the current method. These technologies might enable more complicated actuation such as hands motion or direction-controlled movement by incorporating a liquid metal spring inside the gel for local control. At present, fabrication by the processing of a temperature-responsive gel with a 3D printer has been realized.[39] This processing might improve the fabrication limit of gel actuators. Currently, a variety of issues including the response time of actuation and the requirements relating to water still need to be resolved before practical devices can be developed. Another important aspect is the response time of the actuation. This factor can be improved by reducing the size, reducing the crosslink density,[40] and grafting the same linear PNIPAM polymer onto the network main chain.[41] Despite some challenges, the proposed actuator remains a very feasible proposition for realizing underwater, mobile soft robots, and mimicking artificial aquatic plants. As discussed previously, the gel actuators are ultrasoft, can be miniaturized, and can be controlled by electricity. As potential applications, it is expected that these actuators will be used in the medical field, especially in future applications to active catheters and microgrippers in cells. This work presents an important step that extends the potential range of applications of hydrogels as well as the functionality of hydrogel actuators.

Experimental Section

Fabrication Process of the Liquid Metal Spring: The fabrication of gel springs with a core–shell structure was based on the microfluidic method according to the procedures established in the literature. Briefly, the microfluidic device consisted of coaxially aligned nozzles and a needle. As shown in Figure 1b(i), a double nozzle was prepared using a 3D printer (AGIRISTA-3200, KEYENCE) and a syringe needle (NN-1838S, TERUMO) with an inner diameter of 910 μm was attached to the nozzle. Sodium alginate solution, 4 w/w%, was injected from the outer portion, and PVA aqueous solution (Arabic Yamato Standard, YAMATO Co., Ltd.) was injected from inner part. In this study, the PVA aqueous solution was used in the core part because the liquid metal, Galinstan, replaced the core structure inside the spring. The volumetric flow rates of the inner

**ADVANCED
SCIENCE NEWS**

www.advancedsciencenews.com

**ADVANCED
INTELLIGENT
SYSTEMS**

www.advintellsyst.com

and outer solutions were 0.06 and 0.25 mL min^{-1}, respectively. The solutions of PVA and gel were extruded into 2 mol L^{-1} of calcium chloride from an inclined nozzle. An imbalance in the gelation occurred due to the difference in setting speeds between the outside and inside of the inclination. Finally, liquid metal was injected into the core part to replace the PVA aqueous solution with liquid metal.

Fabrication Process of the Gel Actuator with a Liquid Metal Spring: For the telescopic gel actuator, a rod composed of PNIPAM gel was used for actuation. A 5.5 w/w% solution of PNIPAM, 0.1 w/w% of *N,N'*-methylenebisacrylamide (BIS), 5 w/w% of sodium alginate, and 0.24 v/v% of *N,N,N',N'*-tetramethylethylenediamine (TEMED) were mixed with a stirrer. As soon as 0.2 w/w% of ammonium peroxodisulfate (APS) was added to the solution, the aqueous pregel solution was injected into the 3D-printed molds. After 1 h, at room temperature, the mold containing the gel was immersed in a calcium chloride solution to obtain higher robustness of the gel. The gel rod was detached from the mold after 24 h.

For the bending gel actuator, a bilayer structure hydrogel rod was fabricated. An 8.8 w/w% solution of acrylamide, 0.1 w/w% of BIS, 5 w/w% of sodium alginate, and 0.24 v/v% of TEMED were mixed with a stirrer. As soon as 0.2 w/w% of APS was added to the solution, the aqueous solution was poured into a styrene case of thickness 1 mm and sealed with a glass plate covered previously. After 1 h, the PNIPAM gel used in the shrinkage actuator was poured into a 1.4 mm-thick styrene case, covered with a glass plate, and similarly left for 1 h as before. The completed bilayer sheet was immersed in a 0.2 mol L^{-1} aqueous solution of calcium chloride for 24 h to obtain an acrylamide and PNIPAM bilayer sheet. The shape of the gel rod was obtained by pressing with a 3D printer. Eventually, the actuator was completed by wrapping the gel spring around the gel rod.

Mechanical and Electrical Evaluation of the Liquid Metal Spring: To measure the spring constant, an electronic balance (HTR-220, Shinko Denshi) and vertical movement stage (TSD-1003, SIGMAKOKI) were used. A weight was attached to one end of the spring and put on the balance, whereas the other end of the spring was pulled vertically by the vertical movement stage. During the tension of the spring, the weight was monitored on the display of an electric balance. Based on this measurement, the spring constant was calculated.

For the evaluation of the electrical characteristics of the spring, copper wires were inserted into the liquid metal of the spring to achieve an electrical connection to the spring. An LCR meter (ZM2376, NF Corporation) was used for the detection of resistance in both AC and DC.

Locally Controlled Gel Actuation by Resistive Heating of a Liquid Metal Spring: The experiments were performed in water at 22 °C because of the mechanism of PNIPAM actuation. Copper wires were connected to both ends of the liquid metal spring. To drive the 3.5 W DC power supply for 15 min, a power supply (PAN35-5A, Kikusui Electronics) was used. The temperature distribution before and after heat generation was measured with a thermal camera (TA410FC, FLIR Systems). The gel rods of dual or triple actuators were fabricated in the same manner as that of the single gel actuator with a liquid metal spring. After obtaining the rods, the springs were assembled into the rods. Each spring was connected to a power supply. The straight part of the gel rod was defined as the length of the rod. The shrinkage ratio was calculated based on the lengths.

Supporting Information

Supporting Information is available from the Wiley Online Library or from the author.

Acknowledgements

Conflict of Interest

The authors declare no conflict of interest.

[1] H. Ko, Z. Zhang, Y. L. Chueh, E. Saiz, A. Javey, *Angew. Chem. Int. Ed.* **2010**, *49*, 616.
[2] M. M. Hamedi, V. E. Campbell, P. Rothemund, F. Güder, D. C. Christodouleas, J. F. Bloch, G. M. Whitesides, *Adv. Funct. Mater.* **2016**, *26*, 2446.
[3] M. L. O'Grady, P. L. Kuo, K. K. Parker, *ACS Appl. Mater. Interfaces* **2010**, *2*, 343.
[4] E. L. White, J. C. Case, R. Kramer-Bottiglio, *Soft Robot.* **2018**, *5*, 36.
[5] J. K. Paik, E. Hawkes, R. J. Wood, *Smart Mater. Struct.* **2010**, *19*, 125014.
[6] J. K. Paik, R. J. Wood, *Smart Mater. Struct.* **2012**, *21*, 065013.
[7] E. Torres-Jara, K. Gilpin, J. Karges, R. J. Wood, D. Rus, *IEEE Robot. Autom. Mag.* **2010**, *17*, 78.
[8] S. Takeuchi, I. Shimoyama, in *Proc. of 1st Annual Int. IEEE-EMBS Special Topics Conf. on Microtechnologies in Medicine Biology* **2000**, Vol. *51*, p. 491.
[9] S. Takeuchi, I. Shimoyama, *J. Microelectromech. Syst.* **2000**, *9*, 24.
[10] S. J. A. Koh, T. Li, J. Zhou, X. Zhao, W. Hong, J. Zhu, Z. Suo, *J. Polym. Sci. B: Polym. Phys.* **2011**, *49*, 504.
[11] P. Gupta, K. Vermani, S. Garg, *Drug Discov. Today* **2002**, *7*, 569.
[12] X. Z. Zhang, R. X. Zhuo, J. Z. Cui, J. T. Zhang, *Int. J. Pharm.* **2002**, *235*, 43.
[13] M. Das, S. Mardyani, W. C. W. Chan, E. Kumacheva, *Adv. Mater.* **2006**, *18*, 80.
[14] M. Bassil, J. Davenas, M. E. L. Tahchi, *Sens. Actuators B* **2008**, *134*, 496.
[15] D. Kaneko, P. G. Jian, Y. Osada, *J. Mater. Chem.* **2002**, *12*, 2169.
[16] Y. Haraguchi, T. Shimizu, M. Yamato, T. Okano, *RSC Adv.* **2012**, *2*, 2184.
[17] H. Suzuki, *J. Intell. Mater. Syst. Struct.* **2006**, *17*, 1091.
[18] Q. Yu, J. M. Bauer, J. S. Moore, D. J. Beebe, *Appl. Phys. Lett.* **2001**, *78*, 2589.
[19] S. Liu, E. Boatti, K. Bertoldi, R. Kramer-Bottiglio, *Extrem. Mech. Lett.* **2018**, *21*, 35.
[20] A. Sydney Gladman, E. A. Matsumoto, R. G. Nuzzo, L. Mahadevan, J. A. Lewis, *Nat. Mater.* **2016**, *15*, 413.
[21] E. Reyssat, L. Mahadevan, *J. R. Soc. Interface* **2009**, *6*, 951.
[22] Z. L. Wu, M. Moshe, J. Greener, H. Therien-Aubin, Z. Nie, E. Sharon, E. Kumacheva, *Nat. Commun.* **2013**, *4*, 1.
[23] G. H. Kwon, J. Y. Park, J. Y. Kim, M. L. Frisk, D. J. Beebe, S. H. Lee, *Small* **2008**, *4*, 2148.
[24] T. Fujigaya, T. Morimoto, Y. Niidome, N. Nakashima, *Adv. Mater.* **2008**, *20*, 3610.
[25] N. Terasawa, N. Ono, K. Mukai, T. Koga, N. Higashi, K. Asaka, *Carbon* **2012**, *50*, 311.
[26] M. Zrínyi, J. Fehér, G. Filipcsei, *Macromolecules* **2000**, *33*, 5752.
[27] C. Yao, Z. Liu, C. Yang, W. Wang, X. J. Ju, R. Xie, L. Y. Chu, *Adv. Funct. Mater.* **2015**, *25*, 2980.
[28] B. Xu, H. Jiang, H. Li, G. Zhang, Q. Zhang, *RSC Adv.* **2015**, *5*, 13167.

[29] W. J. Zheng, N. An, J. H. Yang, J. Zhou, Y. M. Chen, *ACS Appl. Mater. Interfaces* **2015**, *7*, 1758.

[30] D. Morales, I. Podolsky, R. W. Mailen, T. Shay, M. D. Dickey, O. D. Velev, *Micromachines* **2016**, *7*, 98.

[31] E. Palleau, D. Morales, M. D. Dickey, O. D. Velev, *Nat. Commun.* **2013**, *4*, 1.

[32] C. Pacchierotti, F. Ongaro, F. Van Den Brink, C. Yoon, D. Prattichizzo, D. H. Gracias, S. Misra, *IEEE Trans. Autom. Sci. Eng.* **2018**, *15*, 290.

[33] D. Morales, E. Palleau, M. D. Dickey, O. D. Velev, *Soft Matter* **2014**, *10*, 1337.

[34] Y. S. Kim, M. Liu, Y. Ishida, Y. Ebina, M. Osada, T. Sasaki, T. Hikima, M. Takata, T. Aida, *Nat. Mater.* **2015**, *14*, 1002.

[35] X. Zhang, C. L. Pint, M. H. Lee, B. E. Schubert, A. Jamshidi, K. Takei, H. Ko, A. Gillies, R. Bardhan, J. J. Urban, M. Wu, R. Fearing, A. Javey, *Nano Lett.* **2011**, *11*, 3239.

[36] E. Wang, M. S. Desai, S. W. Lee, *Nano Lett.* **2013**, *13*, 2826.

[37] C. H. Zhu, Y. Lu, J. Peng, J. F. Chen, S. H. Yu, *Adv. Funct. Mater.* **2012**, *22*, 4017.

[38] K. Yoshida, H. Onoe, *Sci. Rep.* **2017**, *7*, 1.

[39] D. Han, Z. Lu, S. A. Chester, H. Lee, *Sci. Rep.* **2018**, *8*, 1.

[40] R. Yoshida, K. Uchida, Y. Kaneko, K. Sakai, A. Kikuchi, Y. Sakurai, T. Okano, *Nature* **1995**, *374*, 240.

[41] Y. Kaneko, K. Sakai, A. Kikuchi, R. Yoshida, Y. Sakurai, T. Okano, *Macromolecules* **1995**, *28*, 7717.

Supporting Information

Hydrogel actuator with a built-in stimulator using liquid metal for local control

Ken Matsubara[1], Daiki Tachibana[1], Ryosuke Matsuda[1], Hiroaki Onoe[2], Ohmi Fuchiwaki[1,3], Hiroki Ota[1,3]*

[1]Department of Mechanical Engineering, Yokohama National University, 79-5 Tokiwadai, Hodogaya-ku, Yokohama, 240-8501, Japan
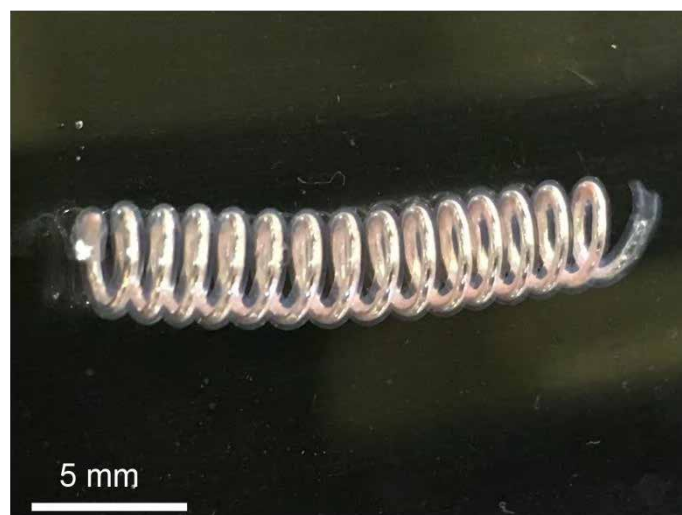[2]Graduate School of Environment and Information Science, Yokohama National University, 79-5 Tokiwadai, Hodogaya-ku, Yokohama, 240-8501, Japan
[3]Department of Chemistry and Biotechnology, Yokohama National University, 79-5 Tokiwadai, Hodogaya-ku, Yokohama, 240-8501, Japan
[4]Department of Mechanical Engineering, Keio University, 3-14-1 Hiyoshi, Kohoku-ku, Yokhama, 223-8522, Japan
[5]Graduate School of System Integration, Yokohama National University, 79-5 Tokiwadai, Hodogaya-ku, Yokohama 240-8501, Japan

*Corresponding author

Figure S1 Fabricated hydrogel spring with liquid metal

a

i

Spacer   Acrylamide gel Glass plate

1 mm

ii

iii

PNIPAM gel

1.4 mm

vii

Punch

vi

CaCl$_2$

v

b

Heat
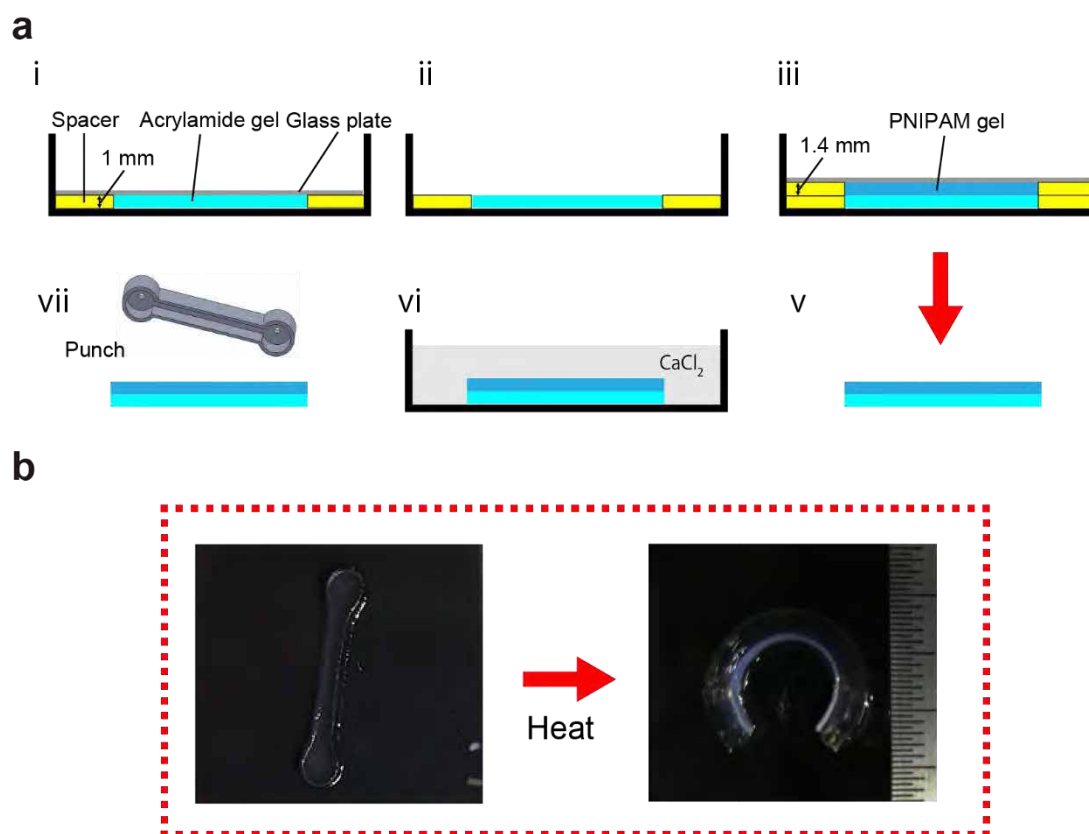
Figure S2. Bilayered hydrogel rods. a. Fabrication of the bilayered rod. The acrylamide gel is formed by a 3D printed spacer (i, ii). The PNIPAM gel is polymerized onto the acrylamide gel (iii), and a 3D printed punch shapes the rod. To obtain higher robustness for the gel, the hydrogel is dipped in a CaCl$_2$ solution (iv). Finally, the hydrogel rod is collected (v). **b.** Demonstration of the bending actuation.

a

b
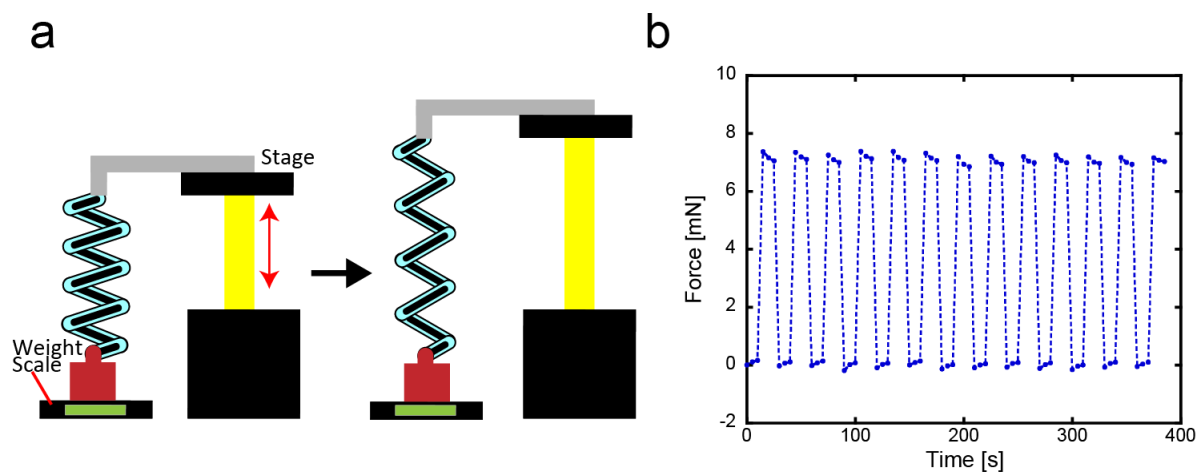

Figure S3 Repeatability test of mechanical characteristic by stretching. a. Experimental
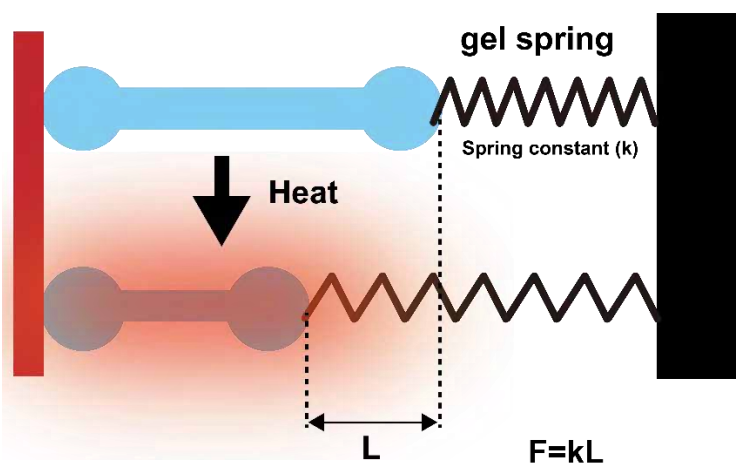
set-up. **b.** Result of the repeatability test.
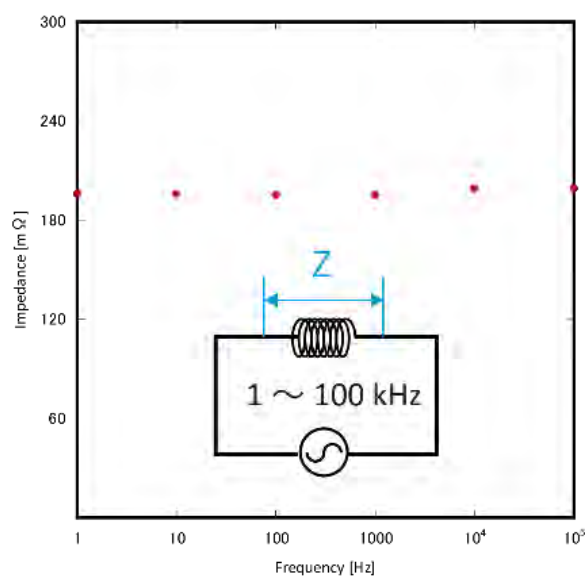
Figure S4. Impedance change with respect to frequency of AC. The impedance was stable
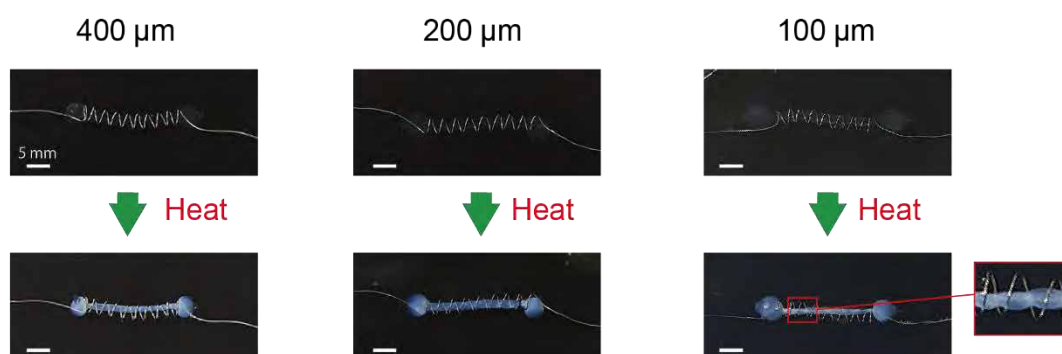
in AC from 1 Hz to 10^5 Hz.

a

Heat

b

Heat

5 mm
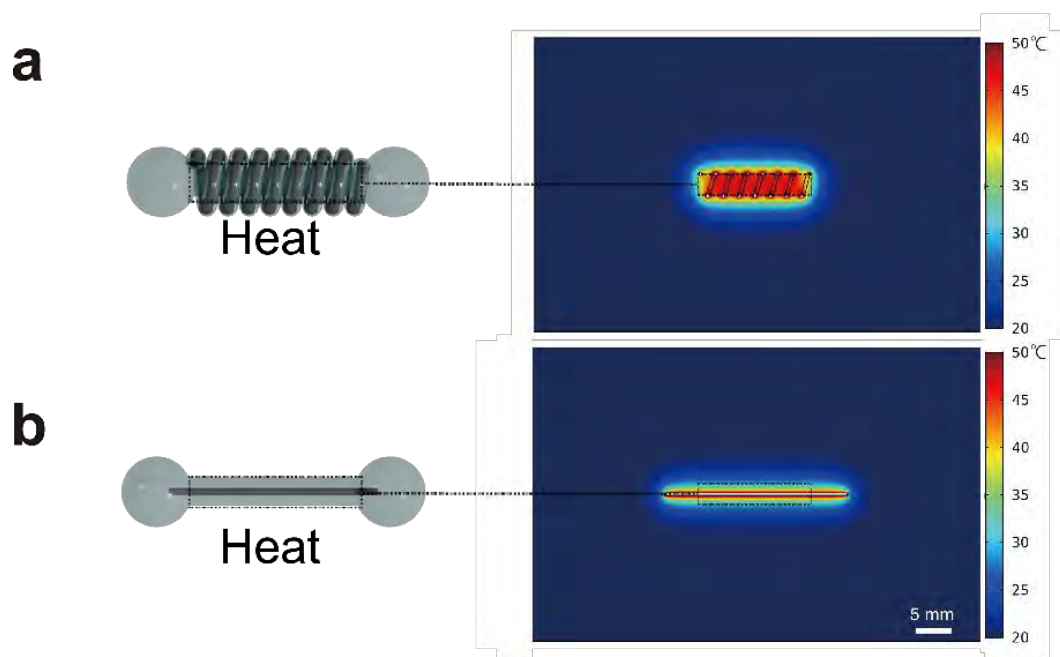
Figure S5. Heat distribution around a liquid metal channel by thermal simulation. a.

spiral structure and **b.** straight structure of liquid channnls.
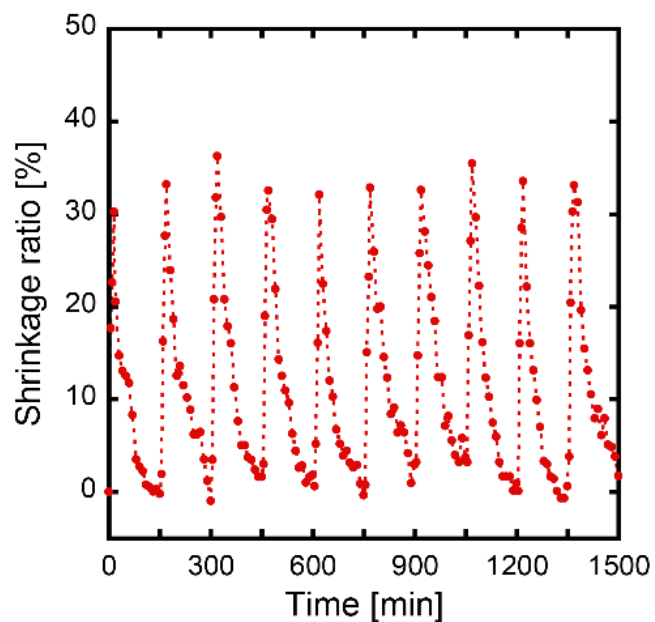
Figure S6. Repeatability test of hydrogel shrinkage.

Figure S7 experimental set-up of the driving force of the thermo-responsive gel.

Figure S8. Hydrogel actuator composed of a PNIPAM rod and solid-state metal springs.

The actuators with helical wiring in the range 400–100 μm could not work.

Table S1 the relationship between mechanical properties and materials of stimulators

	Actuator using liquid metal	Actuator using nichrome wire		
Wire diameter [μm]	607	400	200	100
Shrinkage ratio [%]	36	0	0	0
Spring constant [N/m]	0.71	797	61.0	5.73